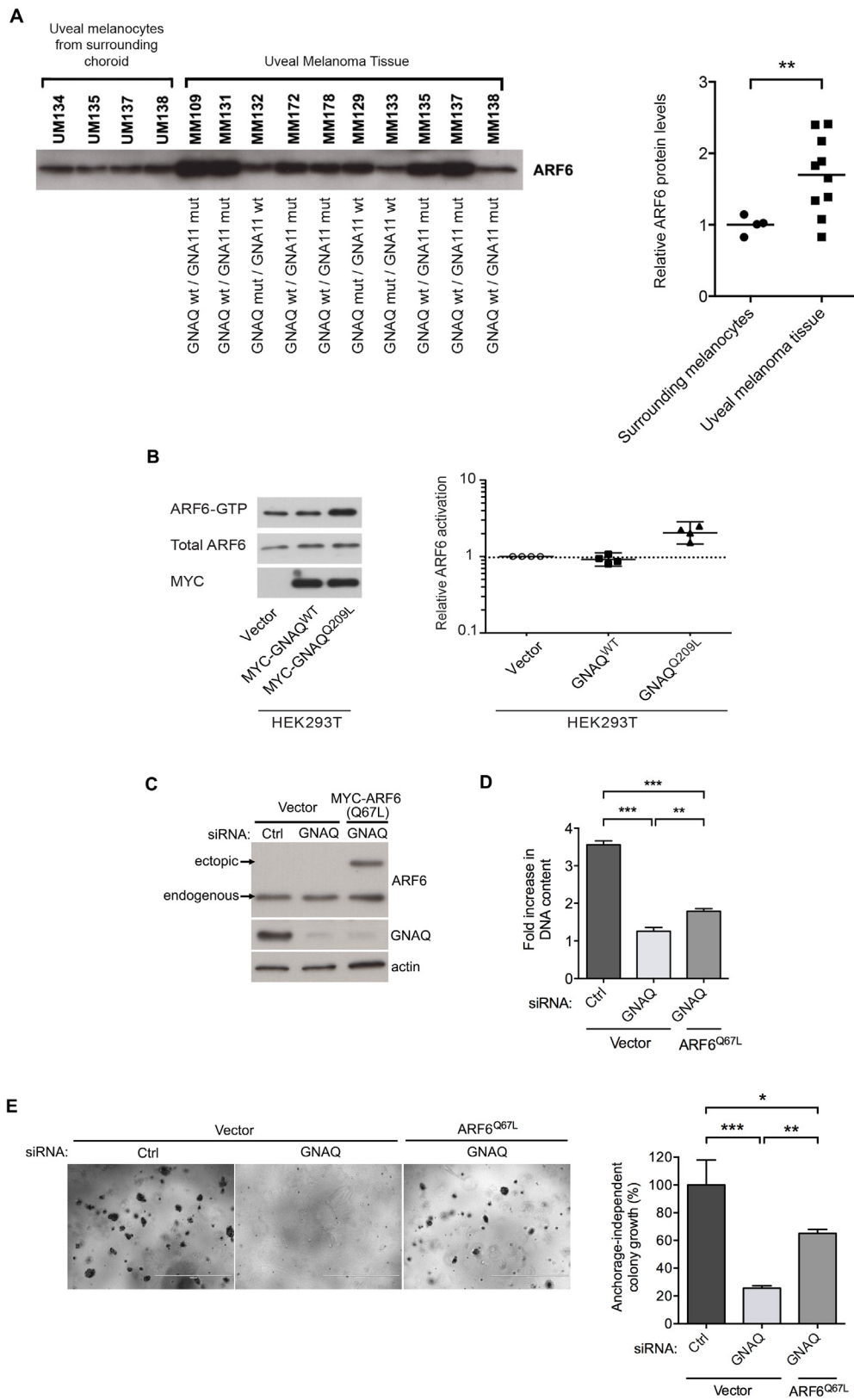


SUPPLEMENTAL DATA



**Figure S1. Related to Figure 1. Constitutively active ARF6 partially rescues GNAQ knockdown in uveal melanoma cells.**

(A) ARF6 protein levels in human uveal melanomas and in melanocytes from surrounding normal choroid tissues. ARF6 expression levels were normalized to total protein (15  $\mu$ g of protein loaded per sample). Data for each normal melanocyte or tumor sample is shown in the graph with mean illustrated by horizontal bar. \*\* $p < 0.01$ . Welch's t-test.  $n = 4$  and 10. *GNAQ* and *GNA11* mutational status is shown for each tumor (WT = wild type; Mut = activating mutation).

(B) Immunoblot of ARF6-GTP pull-downs from HEK293T cells that were transfected with MYC-tagged *GNAQ*<sup>Q209L</sup> or MYC-tagged wild-type (WT) *GNAQ*.

The graph shows individual data points normalized to control along with geometric means and 95% confidence intervals (95% CI). 95% CIs that do not cross the dotted line at  $y=1$  represent significant differences relative to the control at  $\alpha=0.05$ .  $n=4$ .

(C) Immunoblot of lysates prepared from Mel202 cells transfected with empty vector or MYC-ARF6<sup>Q67L</sup> and treated with Control (Ctrl) or *GNAQ* siRNAs. Knockdown of *GNAQ* and expression of endogenous (wild-type) and ectopic (MYC-ARF6<sup>Q67L</sup>) ARF6 were evaluated by immunoblotting. Actin was used as a loading control. Knockdown of *GNAQ* and ectopic expression of ARF6<sup>Q67L</sup> were checked for each of the three proliferation and anchorage-independent colony growth experiments shown in panels D and E.

(D) Cell proliferation as monitored by DNA content using CyQUANT reagent and a fluorescent microplate reader. Mel202 cells were treated as described for panel C.  $n=3$ .

(E) Anchorage-independent colony growth as monitored microscopically and by DNA content using CyQUANT reagent and a fluorescent microplate reader. Mel202 cells were treated as described for panel C. Scale bar: 1000  $\mu\text{m}$ .

For panels D and E, data are represented as mean  $\pm$  SD,  $n=3$  experiments. One-way ANOVA, Tukey's multiple comparisons test, \* $p<0.05$ , \*\* $p<0.01$ , \*\*\* $p<0.001$ .

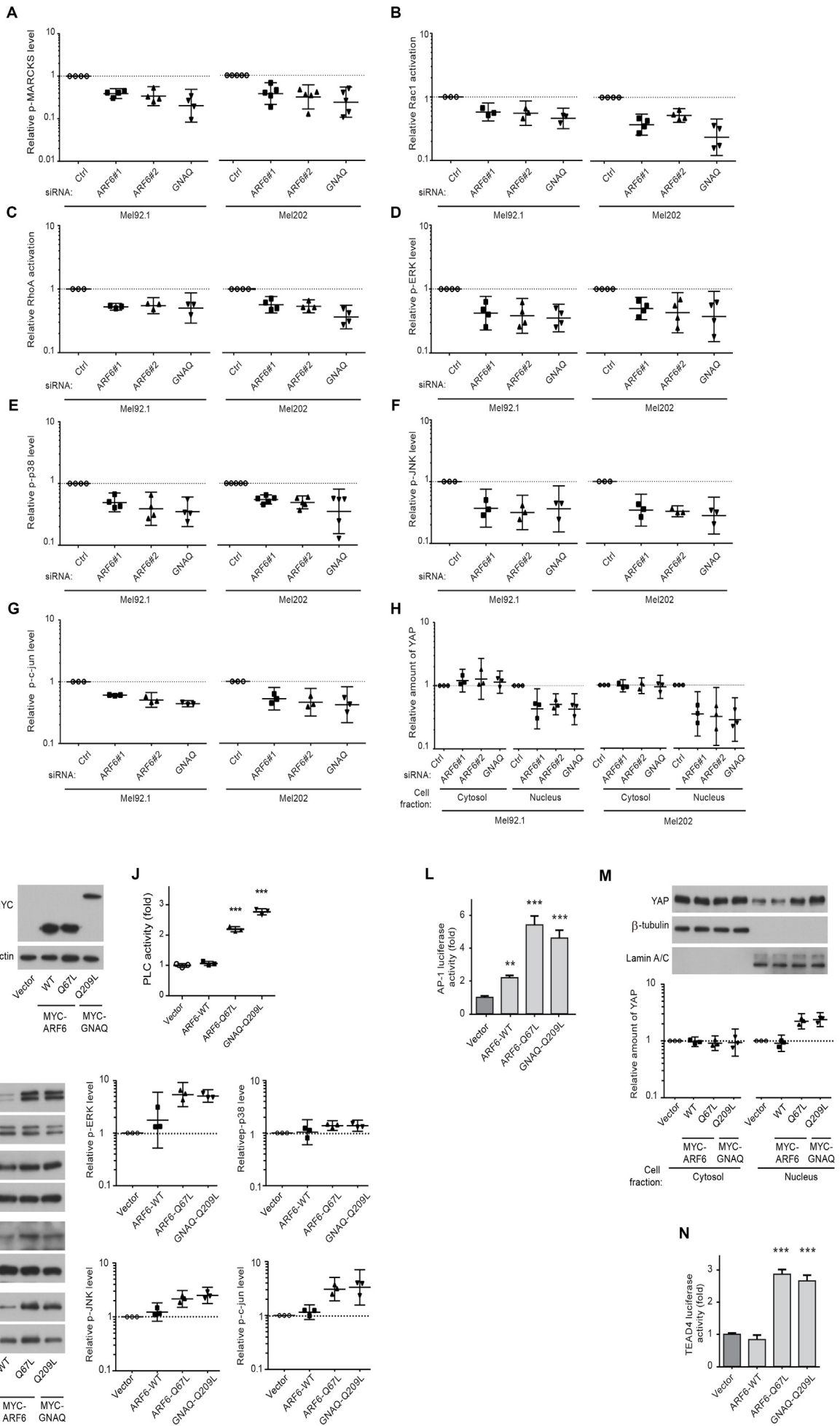


**Figure S2. Related to Figure 2. Quantitation of western blots; Ectopic expression of constitutively active ARF6 (ARF6<sup>Q67L</sup>) in HEK293T cells activates downstream oncogenic GNAQ signaling pathways.**

(A-H) Quantitation of the activation of MARCKS (G), Rac1 (H), RhoA (I), ERK (J), p38 (K), JNK (L), c-jun (M), and the subcellular localization of YAP (N) from the immunoblots shown in Figure 2.

For panels B, D, and F, the data are represented as mean  $\pm$  SD, n=3 experiments. One-way ANOVA, Dunnett's multiple comparisons test, \*\*\*p < 0.001. For panels C, E, and G-N, the graphs show individual data points normalized to control along with geometric means and 95% confidence intervals (95% CI). 95% CIs that do not cross the dotted line at y=1 represent significant differences relative to the control at  $\alpha=0.05$ . n=3 to 5 as indicated.

(I-N) All results are following the transfection of empty vector, MYC-tagged wild-type (WT) ARF6, MYC-tagged ARF6<sup>Q67L</sup>, or MYC-tagged GNAQ<sup>Q209L</sup> in HEK293T cells.

(I) Immunoblot showing that MYC-ARF6<sup>WT</sup>, MYC-ARF6<sup>Q67L</sup>, or MYC-GNAQ<sup>Q209L</sup> is expressed in HEK293T cells following transfection.

(J) PLC activity in a phosphoinositide turnover assay.

(K) Immunoblots of phosphorylated (p) ERK, p38, JNK, and c-jun.

(L) Graph illustrating AP-1-mediated transcriptional activity in a luciferase reporter assay.

(M) Immunoblots and quantitation showing the subcellular fractionation of YAP.

(N) Graph illustrating YAP-mediated transcriptional activity in a luciferase reporter assay.

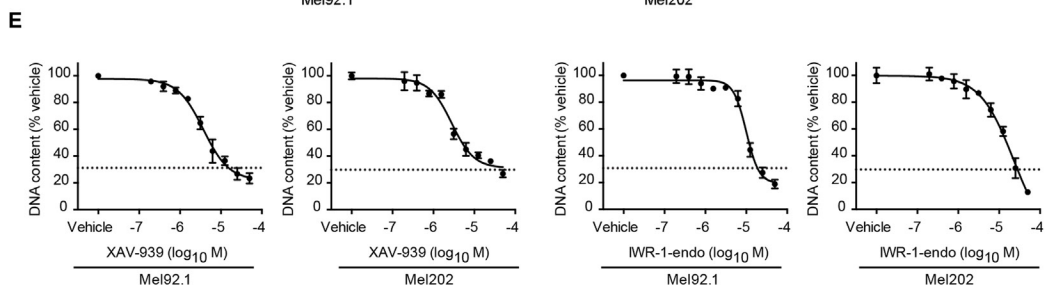
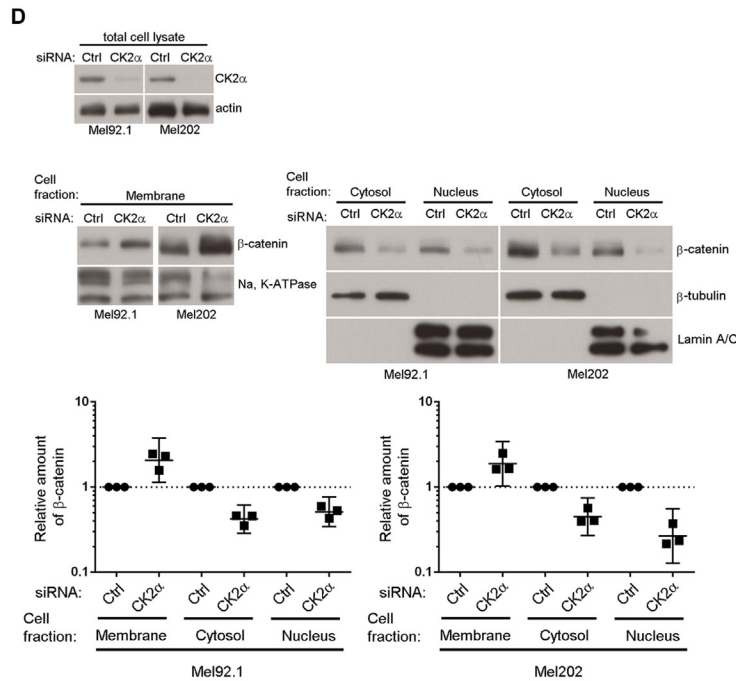
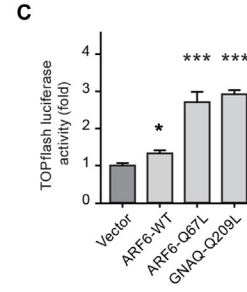
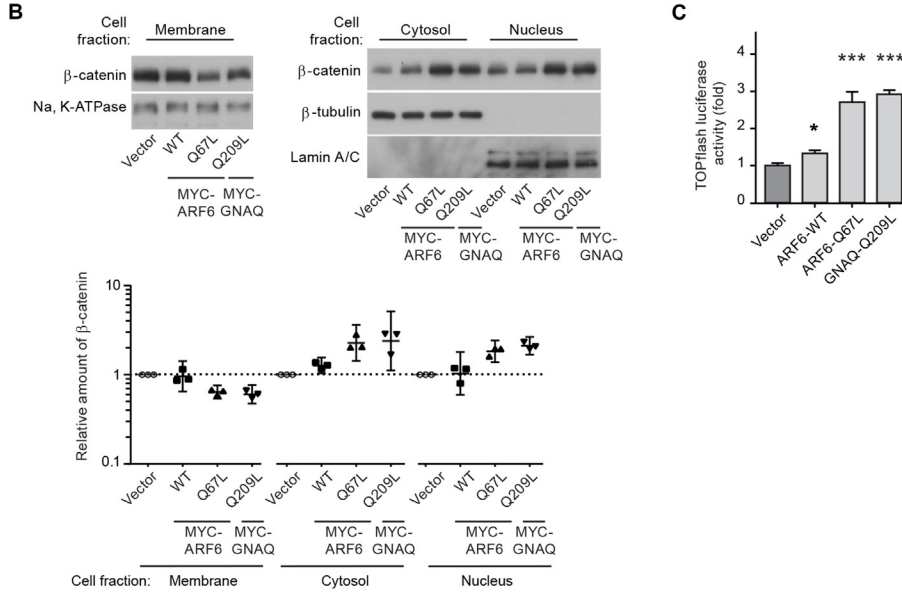
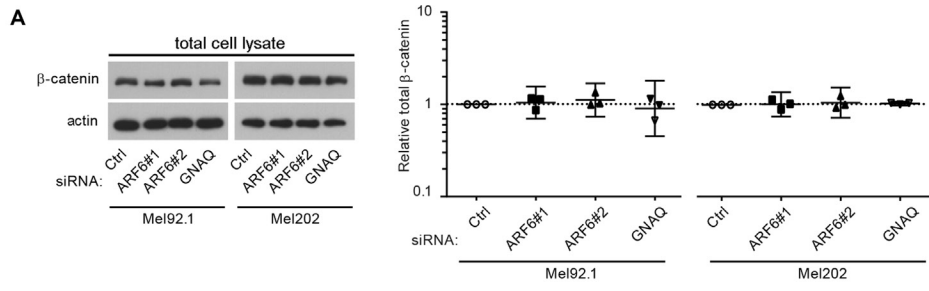


**Figure S3. Related to Figure 3. Elucidating the GNAQ<sup>Q209L</sup>-ARF6 signaling pathway that leads to  $\beta$ -catenin-mediated transcription and proliferation in uveal melanoma.**

(A) Immunoblots examining total  $\beta$ -catenin protein levels in Mel92.1 and Mel202 cells following treatment with ARF6#1, ARF6#2, GNAQ, or control (Ctrl) siRNAs and quantitation of the immunoblots.

(B) Immunoblots showing the subcellular fractionation of  $\beta$ -catenin following transfection of HEK293T cells with empty vector, MYC-tagged wild-type (WT) ARF6, MYC-tagged ARF6<sup>Q67L</sup>, or MYC-tagged GNAQ<sup>Q209L</sup> and quantitation of the immunoblots. The graph shows individual data points normalized to control along with geometric means and 95% confidence intervals (95% CI). 95% CIs that do not cross the dotted line at  $y=1$  represent significant differences relative to the control at  $\alpha=0.05$ .  $n=3$ .

(C)  $\beta$ -catenin-mediated transcriptional activity in a luciferase reporter assays following transfection of HEK293T cells with empty vector, MYC-tagged ARF6<sup>WT</sup>, MYC-tagged ARF6<sup>Q67L</sup>, or MYC-tagged GNAQ<sup>Q209L</sup>. The data are represented as mean  $\pm$  SD,  $n=3$  experiments. One-way ANOVA, Dunnett's multiple comparisons test, \* $p < 0.05$ , \*\*\* $p < 0.001$ .

(D) *Upper panel:* Immunoblots showing CK2 $\alpha$  (catalytic subunit of CK2) knockdown for the subcellular fractionation studies shown in lower panel. *Lower panel:* Subcellular fractionation studies to determine the role of CK2 in controlling  $\beta$ -catenin intracellular location.

(E) Mel92.1 and Mel202 cell proliferation assays following inhibition of  $\beta$ -catenin signaling with XAV939 or IWR-1-endo. Dotted horizontal line represents baseline DNA content before treatment with the inhibitor.  $n=3$ .

For panels A and B, the graphs show individual data points normalized to control along with geometric means and 95% confidence intervals (95% CI). 95% CIs that do not cross the dotted line at  $y=1$  represent significant differences relative to the control at  $\alpha=0.05$ .  $n=3$ .

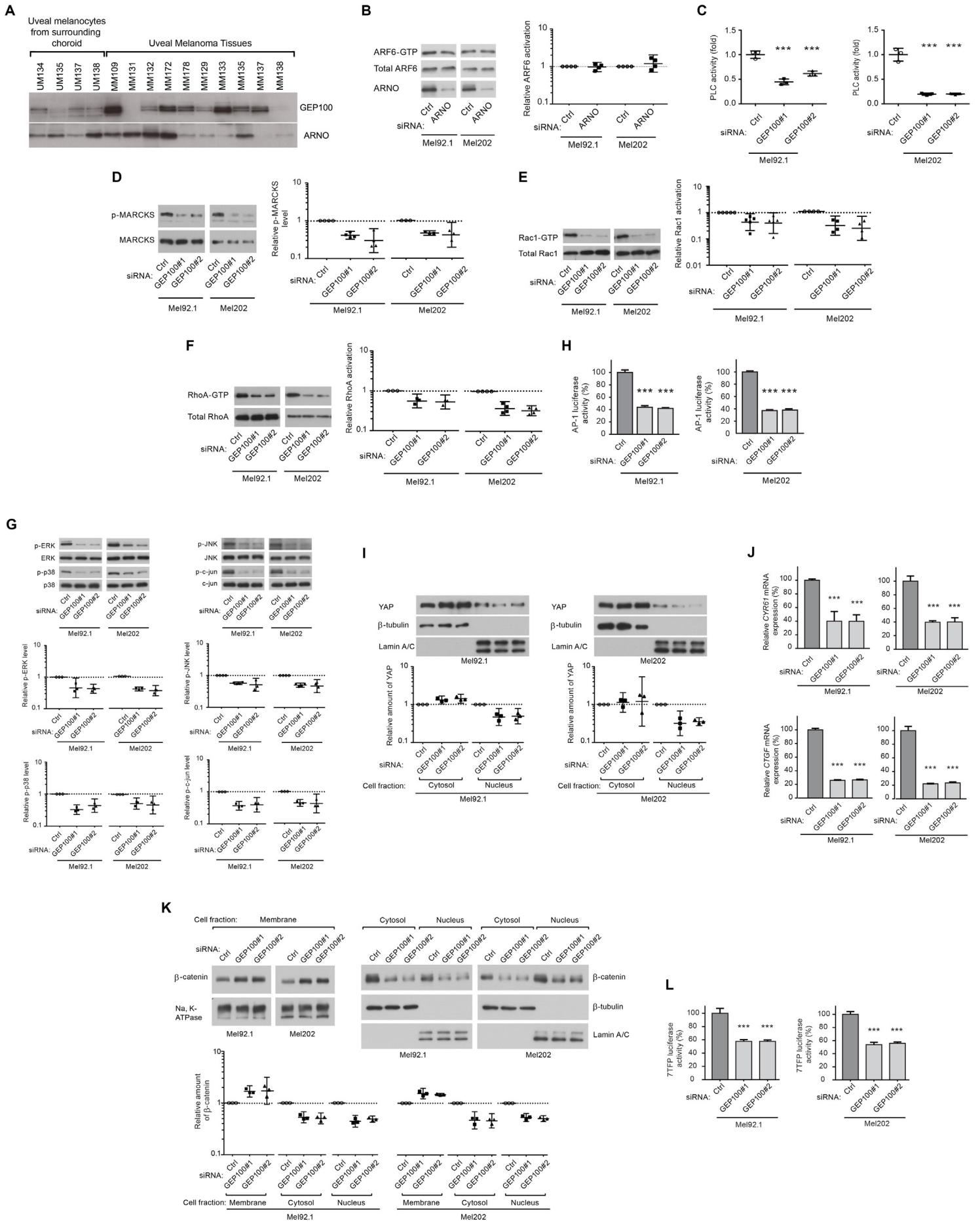


**Figure S4. Related to Figure 4. Silencing of GEP100 inhibits oncogenic GNAQ-induced PLC, Rac/Rho, YAP, and  $\beta$ -catenin signaling in uveal melanoma cells.**

(A) Immunoblots assessing GEP100 and ARNO protein levels in human uveal melanoma tissues and in melanocytes from surrounding normal choroid tissues.

(B) ARF6-GTP pull-downs following treatment of Mel92.1 and Mel202 cells with ARNO or control (Ctrl) siRNA.

(C-G) PLC activity in a phosphoinositide turnover assay (C) and activation of MARCKS (D), Rac1 (E), RhoA (F), and ERK, p38, JNK, and c-jun (G) as measured by immunoblots following treatment of Mel92.1 and Mel202 cells with two independent GEP100 siRNAs (GEP100#1 and GEP100#2) or Ctrl siRNA.

(H) AP-1-mediated transcription in a luciferase activity assay following GEP100 knockdown in Mel92.1 and Mel202 cells.

(I and J) Subcellular fractionation assays of YAP (A) and YAP target-gene mRNA levels (B) following GEP100 silencing in Mel92.1 and Mel202 cells.

(K and L) Subcellular fractionation assays of  $\beta$ -catenin (C) and  $\beta$ -catenin-mediated transcriptional activity in a luciferase reporter assay (D) following GEP100 knockdown in Mel92.1 and Mel202 cell.

For panels B, D-G, I, and K, the graphs show individual data points normalized to control along with geometric means and 95% confidence intervals (95% CI). 95% CIs that do not cross the dotted line at  $y=1$  represent significant differences relative to the control at  $\alpha=0.05$ .  $n=3$  to 5 as indicated. For panels C, H, J, and L, the data are represented as mean  $\pm$  SD,  $n=3$  experiments. One-way ANOVA, Dunnett's multiple comparisons test, \*\*\* $p < 0.001$ .



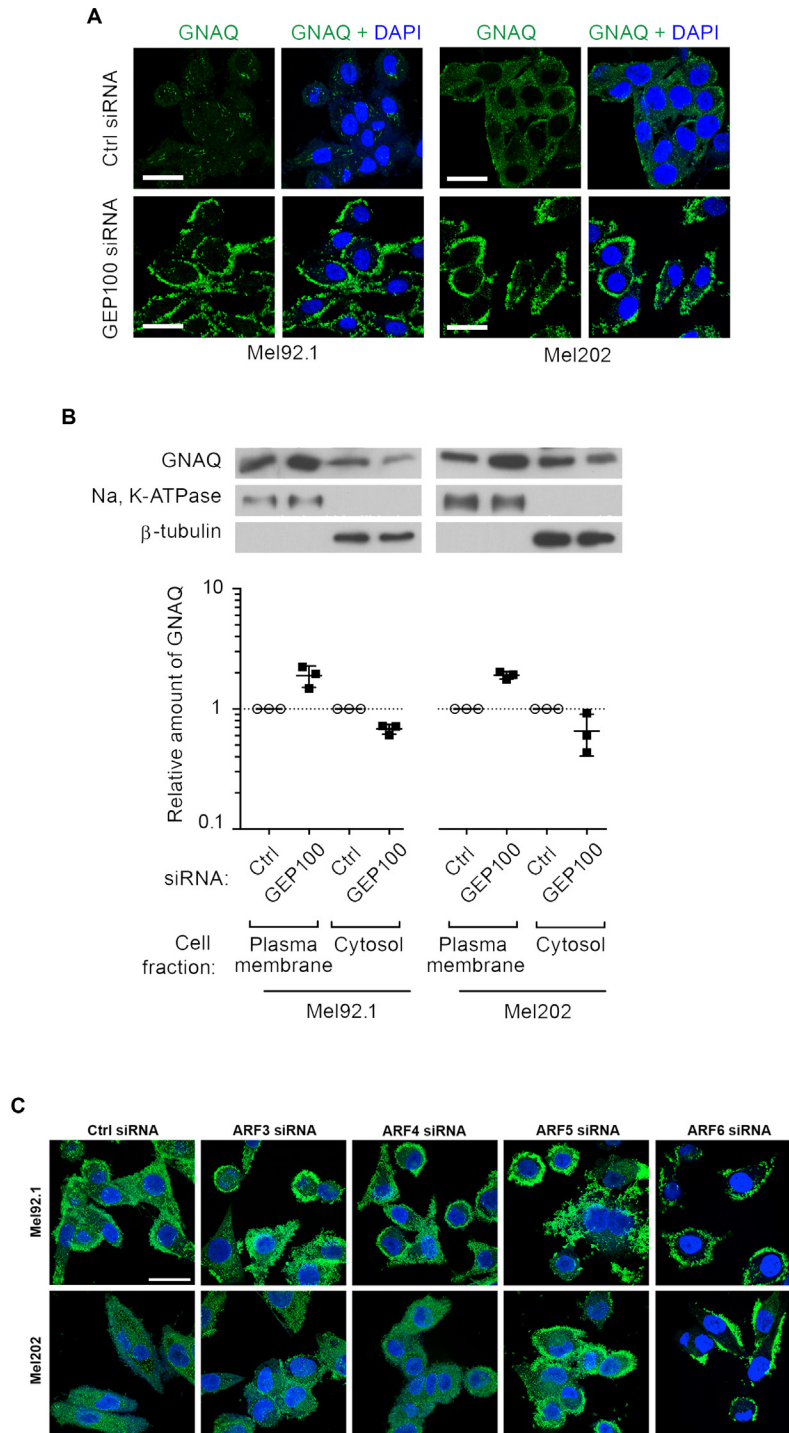


**Figure S5. Related to Figure 5. Knocking down GEP100 or ARF6 but not other ARF family members promotes the localization of GNAQ to the plasma membrane.**

(A and B) Immunocytofluorescent staining (A) and subcellular fractionation (B) of GNAQ in Mel92.1 and Mel202 cells that were transfected with GEP100 or control (Ctrl) siRNA. Scale bar: 30  $\mu$ m.

The graph shows individual data points normalized to control along with geometric means and 95% confidence intervals (95% CI). 95% CIs that do not cross the dotted line at  $y=1$  represent significant differences relative to the control at  $\alpha=0.05$ .  $n=3$ .

(C) Mel 92.1 and Mel202 cells were exposed to siRNAs against *ARF3*, *ARF4*, *ARF5*, or *ARF6*, and subcellular localization of GNAQ was monitored by immunofluorescence. Only *ARF6* knockdown drives GNAQ localization towards the plasma membrane. *ARF1* expression is required for cell viability and therefore its effect on GNAQ localization cannot be assessed. Humans do not possess an *ARF2* gene. Scale bar = 30  $\mu$ m.

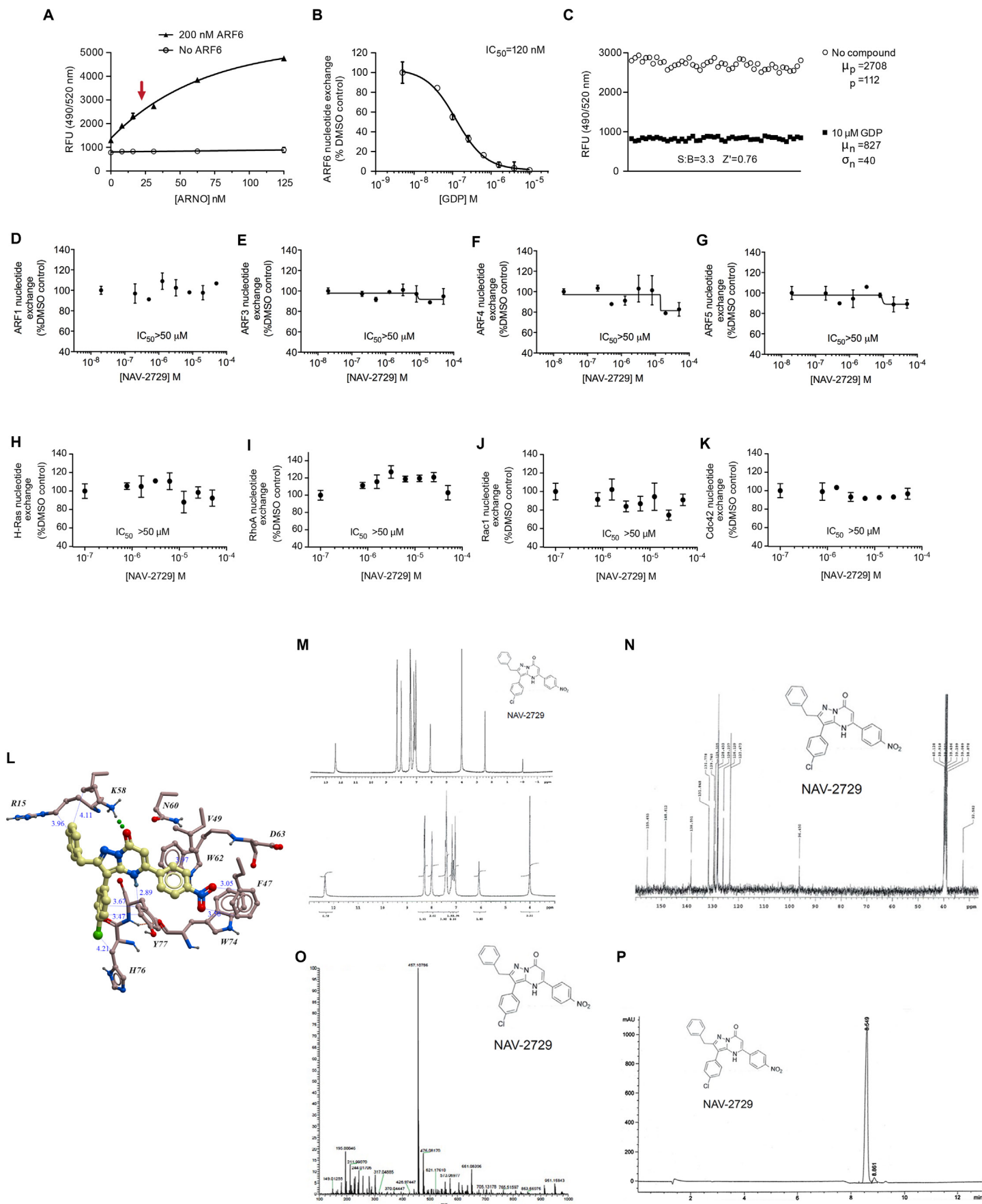


**Figure S6. Related to Figure 6. Development and validation of a fluorometric ARF6 nucleotide exchange assay, assessing the specificity of NAV-2729, and spectral and chromatographic analyses of NAV-2729.**

(A) Dependence of signal intensity on the presence of ARF6 and an ARF-GEF (ARNO). The arrow indicates the concentration of ARNO selected for the assay protocol.

(B) Validation assay using GDP as a reference inhibitor.

(C) Determination of signal-to-background ratio (S:B) and  $Z'$ -factor.

(D-K) Non-inhibitory effects of NAV-2729 for other small GTPases (ARF1, ARF3, ARF4, ARF5, RhoA, Rac1, H-Ras, and Cdc42).

(L) Molecular docking model of NAV-2729 binding to ARF6-ARFGEF complex showing the major interactions of ARF6 residues with the inhibitor.

(M) Proton NMR spectra of NAV-2729.

(N) Carbon-13 spectra of NAV-2729.

(O) High Resolution Mass Spectra of NAV-2729.

(P) HPLC of NAV-2729.

All data are represented by mean  $\pm$  SD.

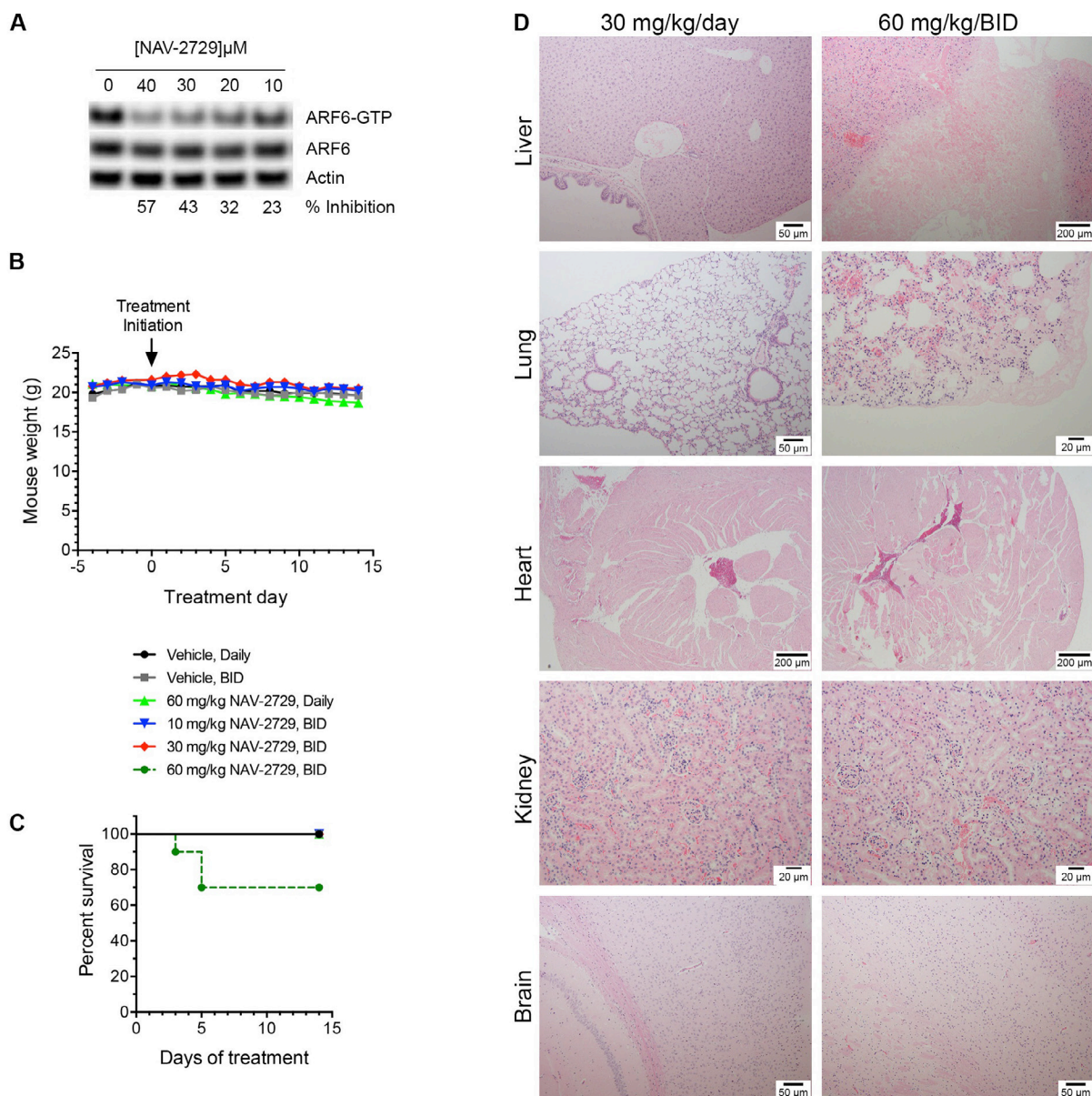


**Figure S7. Related to Figure 8. Therapeutic dosages of NAV-2729 are not toxic to mice.**

(A) ARF6-GTP pull-downs following NAV-2729 treatment of NIH/3T3 cells at the indicated concentrations. Percent inhibition of ARF6 activation is shown below each lane.

(B) Daily mean weights of DBA/1J mice over a 14-day period. Mice were administered NAV-2729 or vehicle by intraperitoneal injection as indicated in the key (n=10; error bars omitted for clarity).

(C) Survival curve shows that all mice survived during a 14-day dosing regimen, except for 3 out of 10 mice that received the highest dosage of NAV-2729 (60 mg/kg, BID). The key is for both panels B and C.

(D) No significant lesions were found in tissues from five major organs collected from C57BL/6J mice that had received daily intraperitoneal injections of 30 mg/kg NAV-2729 (left column). Likewise, no significant lesions were observed in mice that received 30 mg/kg, BID or 60 mg/kg in a single daily injection (see Table S3). However, a large region of necrosis is located in the center of the image of the liver section taken from a mouse that received 60 mg/kg of NAV-2729, BID (right column). Also, the lungs show signs of pneumonia with acute inflammation marked by interstitial neutrophils. Scale bars are shown for each image.

**Table S1. Related to Figure 8. ARF6 inhibition by NAV-2729 is not grossly toxic in multiple strains of mice.**

Dosage		Mouse Strain	# of treatment days	# of mice alive with no signs of morbidity/ Total # of mice
Dose	Frequency, IP			
10 mg/kg	Twice daily	DBA/1J	14	10/10
30 mg/kg*	Once daily	Nude	35	10/10
30 mg/kg	Once daily	C57BL/6J	14	3/3
30 mg/kg	Twice daily	DBA/1J	14	10/10
30 mg/kg	Twice daily	C57BL/6J	14	3/3
60 mg/kg	Once daily	DBA/1J	14	10/10
60 mg/kg	Once daily	C57BL/6J	14	3/3
60 mg/kg	Twice daily	DBA/1J	14	7/10

\*Data taken from the present uveal melanoma study.

IP, intraperitoneal.

**Table S2. Related to Figure 8. Blood analyses for NAV-2729 toxicity study.**

**Once daily intraperitoneal injections**

Blood Cells	Units	Normal range	30 mg/kg, daily			60 mg/kg, daily		
			Mouse 1	Mouse 2	Mouse 3	Mouse 1	Mouse 2	Mouse 3
WBC	K/ $\mu$ L	1.8 - 10.7	7.36	5.20	3.58	8.60	13.26	6.56
RBC	M/ $\mu$ L	6.36 - 9.42	9.02	9.02	8.88	8.20	8.64	8.55
HCT	%	35.1 - 45.4	39.00	36.40	37.50	33.00	35.50	36.50
PLT	K/ $\mu$ L	592 - 2972	831	1036	966	936	913	823

**Twice daily intraperitoneal injections**

Blood Cells	Units	Normal range	30 mg/kg, BID			60 mg/kg, BID		
			Mouse 1	Mouse 2	Mouse 3	Mouse 1*	Mouse 2	Mouse 3
WBC	K/ $\mu$ L	1.8 - 10.7	5.88	5.44	6.76	nd	1.42	6.68
RBC	M/ $\mu$ L	6.36 - 9.42	9.21	8.23	9.89	nd	5.53	8.00
HCT	%	35.1 - 45.4	40.10	36.80	39.20	nd	24.50	33.00
PLT	K/ $\mu$ L	592 - 2972	677	1395	824	nd	97	165

\*nd = not determined, because mouse died at day 7. BID = Twice daily. WBC = White Blood Cell count. RBC = Red Blood Cell count; HCT = Hematocrit; PLT = Platelet count. Red font = high. Blue font = low.

**Table S3. Related to Figure 8. Histopathological analyses for NAV-2729 toxicity study performed by Animal Reference Pathology, a national reference laboratory.**

Mouse #	Tissue	30 mg/kg, Daily IP		60 mg/kg, Daily IP		30 mg/kg, BID IP		60 mg/kg, BID IP	
		No significant lesions	Significant lesions	No significant lesions	Significant lesions	No significant lesions	Significant lesions	No significant lesions	Significant lesions
1	liver	X		X		X			Nec, 2 <sup>c</sup>
	lung	X		X		X			Inf, 2 <sup>c</sup>
	heart	X		X <sup>a</sup>		X		X	
	kidney	X		X		X		X	
	brain	X		X		X		X	
2	liver	X		X		X			Inf, 1 <sup>d</sup>
	lung	X		X		X		X	
	heart	X		X <sup>a</sup>		X		X	
	kidney	X		X		X		X	
	brain	X		X		X		X	
3	liver	X		X		X		X	
	lung	X		X		X		X	
	heart	X <sup>a</sup>		X		X		X	
	kidney	X		X			Inf, 1 <sup>b</sup>	X	
	brain	X		X		X		X	

Type of pathology: Inf-inflammation; Nec-necrosis; other signs of pathology were searched for, including degeneration and neoplasia but none were found, except as noted.

Severity: 1-occasional; 2-mild; 3-moderate; 4-severe

<sup>a</sup> Occasional, subtle degenerative lesions; differential diagnosis includes artifact or cardiac puncture for blood draw.

<sup>b</sup> Single mild area of renal corticomedullary inflammation is probably incidental.

<sup>c</sup> Hepatic necrosis and pneumonia, which is likely indicative of sepsis. Mouse found dead at day 7 of dosing.

<sup>d</sup> Capsular hepatic inflammation, possibly due to intraperitoneal injections.

## SUPPLEMENTAL EXPERIMENTAL PROCEDURES

### Cell lines, proliferation assay, and anchorage-independent colony growth

Mel92.1 and Mel202 uveal melanoma cells were originally obtained from Martine Jager and subsequently characterized in the S.E. Woodman laboratory (Griewank et al., 2012). Mel92.1 and Mel202 uveal melanoma cells were maintained in RPMI 1640 supplemented with 10% fetal bovine serum (FBS). HEK293T cells were purchased from ATCC and maintained in DMEM supplemented with 10% FBS. Cell proliferation assays were performed using CyQUANT (Invitrogen) according to the manufacturer's instructions.  $5 \times 10^3$  uveal melanoma cells were plated into each of three or four wells of a 96-well plate and fluorescence was measured 4 hr later after cell attachment to obtain baseline measurements and at 72 h as endpoint measurements. Anchorage-independent colony growth was quantified by the CytoSelect 96-Well Cell Transformation Assay (Cell Biolabs) as per manufacturer's instructions. After 12-15 days, relative colony size/number was confirmed by microscopic examination and measured by adding CyQUANT reagent to the cultures and measuring fluorescence using a plate reader at excitation/emission wavelengths of 485/530 nm.

### RNA interference, plasmids, transfections, lentiviral transduction, qRT-PCR, and chemicals

All siRNAs, shRNAs, and primer sequences for qRT-PCR are listed in the table below. siRNA duplexes (20 nmol) were transfected into uveal melanoma cells using Lipofectamine RNAiMAX (Invitrogen). Plasmids for wild-type GNAQ and GNAQ<sup>Q209L</sup> were obtained from Missouri S&T cDNA Resource Center. The coding regions of both constructs were re-cloned into pcDNA3.1 vector for MYC epitope-tagging at the N-terminal. For ectopic expression in HEK293T, cells were seeded in 10-cm plates and transfected with the respective plasmids using Lipofectamine LTX (Invitrogen). Lentiviruses containing control and ARF6 shRNA expression constructs were purchased from Sigma and were used to infect Mel202 uveal melanoma cells. Infected cells were selected using 1 µg/ml of puromycin (Invitrogen) for 5 days. For rescue experiments by ARF6<sup>Q67L</sup> during GNAQ knockdown, Mel202 uveal melanoma cells were transfected with pcDNA3.1 as a vector control or ARF6<sup>Q67L</sup> plasmid (Grossmann et al., 2013) and selected with G418 (800 µg/ml; Gibco) for 7 days before transfection with siRNA against GNAQ. qRT-PCR was performed with the Applied Biosystems 7900HT and QuantiTect SYBR Green PCR kit (Qiagen) with the primers listed in the table below. IWR-1-endo and XAV-939 were purchased from Calbiochem.

### RNAi and primer sequences used in this study

Target Gene Symbol	siRNA ID	siRNA Sense Sequence 5' -> 3'	Vendor
Control	AllStars Neg. Control siRNA	Manufacturer's proprietary sequence	QIAGEN
ARF6 #1	SI02757286	ACGUGGAGACGGUGACUUATT	QIAGEN
ARF6 #2	S1565	AGACGGUGACUUACAAAAAtt	AMBION
GNAQ #1	SI02780512	GGACACAUCGUUCGAUUUATT	QIAGEN
GNAQ #2	SI02780988	GGAAUGCUAUGAUAGACGATT	QIAGEN
GEP100 #1	SI03019408	GAAGGGUAGCAGUAAUGAATT	QIAGEN
GEP100 #2	SI04211466	AGAUGAACAAGAACUUCGATT	QIAGEN
ARNO	SI00061299	CGCUGUUGGUAUUCUUUATT	QIAGEN
CK2α	SI02660497	CAUUGAAGCUGAAAUGGUATT	QIAGEN
ARF1	SI00299250	GUGGAAACCGUGGAGUACATT	QIAGEN
ARF3	SI02654477	CCUAUAUGACCAAUCCCUATT	QIAGEN
ARF4	SI04159029	CGUAAAUGAAAUUGGAUATT	QIAGEN
ARF5	SI03242351	CGCGGAUCUUCGGGAAGAATT	QIAGEN

Target Gene Symbol	shRNA ID	Sequence 5' -> 3'	Vendor
Control	SHC002V	CCGGCAACAAGATGAAGAGCACCAACTCGAG TTGGTGTCTTCATCTTGTGTTTTT	SIGMA
ARF6	TRCN0000048005	CCGGGCTCACATGGTTAACCTCTAACTCGAGTTAG AGGTTAACCATGTGAGCTTTTTG	SIGMA

Target Gene for qRT-PCR	Primer Sequence 5' -> 3'
Human GAPDH	(F) GAGTCAACGGATTGGTTCGT
	(R) TTGATTTTGGAGGGATCTCG
Human CTGF	(F) GTTTGGCCCAGACCCAACTA
	(R) GGCTCTGCTTCTCTAGCCTG
Human CYR61	(F) CAGGACTGTGAAGATGCGGT
	(R) GCCTGTAGAAGGGAAACGCT

#### **ARF6/RhoA/Rac1 pull-downs, immunoblots, immunoprecipitation, cell fractionation, PLC assay, luciferase assay, and immunocytofluorescence staining**

ARF6-GTP pull-downs were performed with Arf6 Activation Assay Kit (Cell Biolabs) and RhoA/Rac1-GTP pull-downs were prepared with Rac1 Activation Assay Kit/RhoA Activation Assay Kit (Millipore) according to the manufacturer's instructions.

For immunoblotting and immunoprecipitation, cell lysates were prepared in ice-cold lysis buffer [25 mM HEPES (pH 7.5), 150 mM NaCl, 1% NP-40, 10 mM MgCl<sub>2</sub>, 1 mM EDTA, and 2% glycerol, plus phosphatase and protease inhibitors]. 500 µg of total cell lysates are used for immunoprecipitation. Cell lysates were centrifuged at 14,000 rpm for 10 min, precleared with 40 µl of protein A/G (GE Healthcare) coupled to agarose beads for 3 hours, and then incubated for 1 hour at 4°C with 2.5 µg of GNAQ antibody (Abcam) and protein A/G-agarose beads in a total volume of 1 ml. Immunoprecipitates were washed with ice cold lysis buffer 3 times, resuspended in 40 µl of 2X SDS loading buffer and then boiled for 5 min. Ten micrograms of total cell lysate (2% of the amount used for immunoprecipitation) was used as input, 95% (38 µl) and 5% (2 µl) of each immunoprecipitate were used for assessing the presence of GEP100 and GNAQ, respectively, by immunoblotting. For immunoblotting, primary antibodies were diluted in 5% NFDN or 5% BSA in PBS or TBS plus 0.1% Tween 20 and incubated overnight at 4°C. Plasma membrane or total membrane fraction was isolated with Plasma Membrane Protein Extraction Kit (Abcam) and cytosolic/nuclear fractions were prepared with NE-PER Nuclear and Cytoplasmic Extraction Reagents (Thermo Scientific) according to the manufacturer's instructions. All antibodies for immunoblots, immunoprecipitation, and immunocytofluorescence staining are listed in the table below. Quantification for all immunoblots was by scanning densitometry whereby changes were normalized to loading control, input, and/or total particular protein level, and represents an amalgamation of all independent experimental replicates. Geometric means and 95% confidence intervals were calculated to determine statistically significant changes in protein levels.

#### **Antibodies used in this study**

Antibody Target	Purpose	Vendor	Catalog number	Dilution
ARF6	immunoblot	Millipore	05-1149	1:1,000
GNAQ	immunoblot	Abcam	ab75825	1:3,000
GNAQ	immunocytofluorescence staining	Abcam	ab75825	1:250
GNAQ	immunoprecipitation	Abcam	ab75825	1:278
actin	immunoblot	Cell Signaling Technology	8457	1:5,000
p-MARCKS	immunoblot	Cell Signaling Technology	8722	1:500
MARCKS	immunoblot	Cell Signaling Technology	5607	1:3,000
Rac1	immunoblot	BD Biosciences	610650	1:2,000
RhoA	immunoblot	Cell Signaling Technology	2117	1:1,000
p-ERK	immunoblot	Cell Signaling Technology	4377	1:1,000
ERK	immunoblot	Cell Signaling Technology	9107	1:3,000
p-p38	immunoblot	Cell Signaling Technology	9215	1:1,000
P38	immunoblot	Cell Signaling Technology	8690	1:3,000
p-JNK	immunoblot	Cell Signaling Technology	9255	1:500
JNK	immunoblot	Cell Signaling Technology	9252	1:3,000
p-c-jun	immunoblot	Cell Signaling Technology	3270	1:1,000
c-jun	immunoblot	Cell Signaling Technology	9165	1:3,000



YAP	immunoblot	Cell Signaling Technology	12395	1:3,000
YAP	immunocytofluorescence staining	Cell Signaling Technology	12395	1:400
$\beta$ -tubulin	immunoblot	Santa Cruz Biotechnology	sc-55529	1:1,000
lamin A/C	immunoblot	Cell Signaling Technology	4777	1:5,000
$\beta$ -catenin	immunoblot	BD Biosciences	610154	1:3,000
$\beta$ -catenin	immunocytofluorescence staining	BD Biosciences	610154	1:100
Na, K-ATPase	immunoblot	Cell Signaling Technology	3010	1:500
GEP100	immunoblot	Sigma	G4978	1:3,000
ARNO	immunoblot	Abnova	H00009266-M02	1:500
MYC tag	immunoblot	Cell Signaling Technology	2272	1:3,000
GAPDH	immunoblot	Cell Signaling Technology	2118	1:5,000
CK2 $\alpha$	immunoblot	Cell Signaling Technology	2656	1:1,000
Alexafluor 488-conjugated anti-Mouse IgG	immunocytofluorescence staining	Thermo Fisher Scientific	A-21202	1:200
Alexafluor 488-conjugated anti-Rabbit IgG	immunocytofluorescence staining	Thermo Fisher Scientific	A-21206	1:200
HRP-conjugated anti-Mouse IgG	immunoblot	Jackson ImmunoResearch	715-035-151	1:5,000
HRP-conjugated anti-Rabbit IgG	immunoblot	Jackson ImmunoResearch	111-035-144	1:5,000

$\beta$ -catenin- and AP-1-mediated transcriptional activities in uveal melanoma cells were assayed using lentivirally transduced cells that stably express the TOPflash-based 7TFP luciferase reporter (Addgene) (Fuerer and Nusse, 2010) or AP-1 luciferase reporter (Qiagen). 20-40  $\mu$ g of cell lysates were assayed for firefly luciferase with the Luciferase Assay System (Promega). Luciferase assays for  $\beta$ -catenin, AP-1, and YAP in HEK293T were performed following the transfection of TOPflash, AP-1, or TEAD4 firefly luciferase reporter plasmids (Addgene) and renilla plasmid for a normalized control. Dual luciferases were detected with Dual-Luciferase Reporter Assay System (Promega) according to the manufacturer's instructions.

PLC activity was determined using phosphoinositide turnover assay as previously described (Vaque et al., 2013). Briefly,  $1 \times 10^6$  siRNA-transfected Mel92.1 and Mel202 uveal melanoma cells were seeded into each well of a 6-well plate and  $2 \times 10^5$  HEK293T cells ectopically expressing specific genes following plasmid transfection were plated on each well of a 24-well plate. Cells were incubated with 3  $\mu$ Ci or 1  $\mu$ Ci/well of myo- $^3$ H]-inositol (Perkin Elmer) for 24 h. 10 mM LiCl was added for 20 min to stop the phosphoinositide turnover. 5% TCA was used for cell lysis and the supernatants were applied to an anion-exchange column (Bio-Rad, AG1-X8). Radioactivity in eluted samples was determined with a Beckman scintillation counter.

$3 \times 10^6$  Mel92.1 and Mel202 uveal melanoma cells were plated on 100 mm dishes and transfected using Lipofectamine RNAiMAX (Invitrogen) with siRNAs against ARF6, GEP100, or a control sequence (Qiagen) for 48 h. Transfectants were replated and retransfected for an additional 24 hr in complete medium at a density of  $10^5$  cells/well in 8-well chambered coverglasses coated with 2% 225-bloom Gelatin (EM sciences) in ddH<sub>2</sub>O. After 24 h, monolayers were fixed for 20 minutes in 10% Neutral Buffered Formalin and then washed 3 times in 1x TBS. Antibodies against YAP (1A12) (Cell Signaling),  $\beta$ -catenin (BD Biosciences), and GNAQ (Abcam) were diluted in 1x TBS containing 1% BSA and 0.1% Saponin and applied to cells overnight at 4°C. Wells were rinsed 4 times in 1x TBS, and 10  $\mu$ g/ml Alexafluor 488-conjugated anti-Mouse or anti-Rabbit IgG diluted in 1% BSA /0.1% Saponin was applied for 1 hr at room temperature in a darkened box. Unbound secondary antibody was removed by 4 washes in 1x TBS, and DAPI anti-Fade medium was applied to the drained wells. Fields were randomly selected via the DAPI channel at 1200x with oil immersion. Z-stacked images (4 x 0.5  $\mu$ m slices/field) were taken on an Olympus FV1000 confocal microscope at the University of Utah's Cell Imaging core facility.

The same procedure was also performed on untransfected Mel92.1 and Mel202 that were treated either with 5  $\mu$ M NAV-2729/0.1% DMSO or 0.1% DMSO alone (control) for 1 hr before being fixed and imaged as described above.

### **Human uveal melanoma patient samples**

Primary human uveal melanoma samples were collected and snap frozen at the time of enucleation as previously described (Onken et al., 2007). All samples were confirmed to be uveal melanomas by pathologic evaluation. Normal choroid tissues were also collected from selected enucleated eyes and melanocytes were isolated from these tissues, cultured for 1-3 passages, and frozen as previously described (Matatall et al., 2013). These latter samples served as controls for ARF6 expression analysis. Samples were homogenized and lysed with ice-cold lysis buffer. Lysates were centrifuged for 20 min at 14,000 rpm and the supernatants were used to determine protein concentrations by BCA assays (Pierce). 15  $\mu$ g of lysates were carefully loaded into each well of the gel to generate the immunoblots.

### **Orthotopic xenograft mouse model of uveal melanoma**

All animal studies were performed in accordance with a protocol approved by the University of Utah Institutional Animal Care and Use Committee. Athymic nude mice were purchased from Jackson Laboratories for this study. Mice were anesthetized with an intraperitoneal injection of a mixture of ketamine and xylazine. The eye was viewed under a dissecting microscope, and a sterile 30-gauge needle was used to puncture the posterior chamber of eye.  $10^5$  cells in 5  $\mu$ l were injected into the eye with a Hamilton syringe. For systemic treatment of NAV-2729, the compound was administered daily by intraperitoneal injection of 30 mg/kg over a period of 5 weeks starting on the day of cell injection. After 5 weeks of tumor growth, mice were euthanized with CO<sub>2</sub>, and eyes were collected, fixed, embedded, sectioned, stained with H&E, and examined histologically for primary tumors by a pathologist who was blinded to the treatment regimen.

### **Recombinant Protein Expression and Purification**

All recombinant proteins for the assay development for ARF family members were produced as N-terminally His-tagged fusions in *E. coli* cultures and purified to apparent homogeneity as described previously (Grossmann et al., 2013), including the truncated forms of ARF6 (14-175), ARF1 (18-181), ARF3 (18-181), ARF4 (18-180), and ARF5 (18-180), which do not require membranes or lipid vesicles for full activity, as well as the Sec7 domain-containing fragments of GEP100 and ARNO that encompass residues 391-602 and 50-255, respectively. The recombinant ARF proteins purified in 50 mM Tris-HCl, pH 7.8, 100 mM NaCl, 2 mM MgCl<sub>2</sub>, 10% glycerol, 2 mM  $\beta$ -mercaptoethanol and approximately 150 mM imidazole were routinely converted into GDP-bound form by 2-h incubation in the presence of 5 mM EDTA and GDP in 10-fold molar excess relative to the ARF proteins. Upon addition of MgCl<sub>2</sub> to 20 mM to terminate nucleotide exchange, two rounds of ultrafiltration, using Amicon Ultra-15-10K centrifugal filter units, were performed to remove free nucleotide and replace buffer system with 50 mM Tris-HCl, pH 7.5, 100 mM NaCl, 2 mM MgCl<sub>2</sub>, 10% glycerol, 2 mM  $\beta$ -mercaptoethanol.

### **Toxicity Studies**

C57BL/6J, DBA/1J, or nude mice (J:NU) were administered NAV-2729 by intraperitoneal injection at dosages ranging from 10 mg/kg daily to 60 mg/kg BID (twice daily) over different time courses (14-35 days) and monitored for survival, weight loss/gain, blood cell counts, hematocrit, and/or histopathological changes of the liver, lungs, heart, kidney, and brain. Blood and histopathological analyses were performed by the national veterinary reference laboratories IDEXX Preclinical Research Services (West Sacramento, CA) and Animal Reference Pathology (Salt Lake City UT), respectively.

### **Fluorometric Nucleotide Exchange Assay**

Our fluorometric nucleotide exchange assay for ARF6 and other small GTPases exploits fluorogenic nucleotide probe, GTP labeled with BODIPY FL, for monitoring GDP-to-GTP exchange at the nucleotide-binding site of ARF6. Intrinsic fluorescence of GTP-BODIPY is intramolecularly quenched in the unbound state but is significantly increased upon its binding to the target protein such as ARF6 or other small GTPases (McEwen et al., 2001). The fluorometric ARF6 nucleotide exchange assay used for high-throughput screening and routine inhibition assays was carried out in 96-well format using 100- $\mu$ l aliquots of 50 mM Tris-HCl, pH 7.5, 1 mM MgCl<sub>2</sub>, 0.01% Triton X-100, 2 mM  $\beta$ -mercaptoethanol, 1% DMSO, 50 nM GTP-BODIPY FL, 25 nM ARNO or GEP100, and 200 nM ARF6•GDP (unless indicated otherwise). Replacement of ARF6-bound GDP by GTP-BODIPY FL was monitored by measuring increases in fluorescence intensity during a 30-60 minute time course using a plate reader at the

excitation and emission wavelengths of 490 nm and 520 nm, respectively. The high-throughput screening was performed at the University of Utah Drug Screening Resource using DIVERSet-EXP library of compounds (ChemBridge) at 10  $\mu$ M concentrations. The selectivity tests were conducted in the same format using small GTPases at 200 nM concentrations. Similar to ARF6, all other ARF proteins produced in-house were tested for inhibition in the presence of 25 nM ARNO. Other members of the selectivity panel, namely, RhoA, Rac1, Cdc24, and H-Ras that represent bacterially expressed N-terminally His-tagged full-length recombinant proteins were purchased from Cytoskeleton, Inc., and tested for inhibition of spontaneous nucleotide exchange in the absence of any GEF. GTP-BODIPY FL was provided by Life Technologies. A non-homogeneous version of the above nucleotide exchange assay was employed to assess the mode of ARF6 inhibition with respect to fluorogenic nucleotide. In this case, the recombinant ARF6 was immobilized via its His-tag on the surface of nickel-coated 96-well plates followed by performing nucleotide exchange reaction in the absence or in the presence of NAV-2729 under otherwise standard conditions using GTP-BODIPY FL at the concentrations indicated on Figure 6E. At the end of the reaction period, the microtiter wells were washed three times with both protein- and nucleotide-free assay buffer followed by fluorometric quantification of GTP-BODIPY FL bound to ARF6 as described above. For the determination of signal-to-background ratio (S:B) and  $Z'$ -factor, the assay was performed using a 96-well plate with half of the wells supplemented with 10  $\mu$ M GDP to estimate background fluorescence (B), which is equivalent to mean negative control value ( $\mu$ n), and another half with DMSO control to determine signal intensity (S), which is equivalent to mean positive control value ( $\mu$ p).  $Z'$  factor value was calculated using the following formula:  $Z' = 1 - 3(\sigma_p + \sigma_n)/(\mu_p - \mu_n)$ , which also includes standard deviations for the positive and negative controls ( $\sigma_p$  and  $\sigma_n$ , respectively).

#### Radiometric Nucleotide Exchange Assay

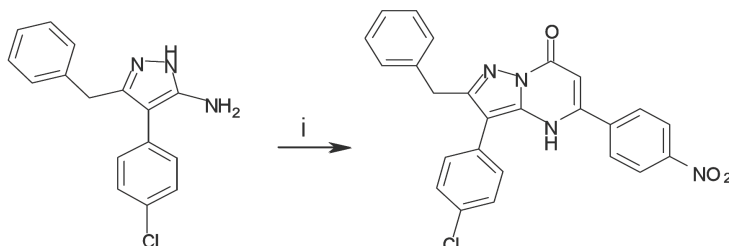
The confirmation of HTS hits using a radiometric assay for ARF6 nucleotide exchange was carried out using 100- $\mu$ l aliquots of same assay mix specified above for the fluorometric technique with the exception that 50 nM [ $^{35}$ S]-GTP $\gamma$ S (2  $\mu$ Ci/ml) was included to replace GTP-BODIPY FL. Upon incubation for 30 minutes in the presence of test articles, 200  $\mu$ l of ice-cold assay buffer supplemented with 10 mM MgCl<sub>2</sub> was added to stop the reaction followed by a rapid vacuum filtration of the samples using a nitrocellulose-bottomed 96-well plate, three washes of the membrane with the above stop solution, and scintillation counting to quantify GTP $\gamma$ S bound to ARF6.

#### Synthetic Methods

All solvents and reagents were purchased from commercial sources and used without further purification unless otherwise noted. Reactions were monitored by TLC (thin layer chromatography) using 0.25 mm silica gel 60 F254 plates purchased from EMD chemicals. Purification was performed with Teledyne ISCO CombiFlash Rf.  $^1$ H NMR and  $^{13}$ C spectra were recorded on a Varian Mercury 400 MHz instrument. Proton chemical shifts are expressed in parts per million (ppm) relative to TMS and calibrated using residual undeuterated solvent as internal reference. High-resolution mass spectra (HRMS) were recorded on Finnigan LTQ-FT, Thermo Electron Corporation. Compound purity was determined by an Agilent HP1050 instrument with a 4.6 mm  $\times$  150 mm Xterra C18 3.5  $\mu$ m column. The flow rate was 1.2 mL/min, and the injection volume was 10  $\mu$ l. HPLC conditions were as follows: mobile phase A, HPLC grade water (0.01% TFA); mobile phase B, HPLC grade acetonitrile (0.01% TFA); UV detector, 254 nm; 95% A/5% B to 0% A/100% B in 10 min, 100% B in 10–11 min, 100% B to 95% A/5% B in 11–13 min, 95% A/5% B in 13–15 min. The final compound was  $\geq$ 95% pure by HPLC.

*Synthesis of 2-benzyl-3-(4-chlorophenyl)-5-(4-nitrophenyl)-4H-pyrazolo[1,5-a]pyrimidin-7-one (NAV-2729)* is described in Scheme shown below. First, we synthesized 3-Benzyl-4-(4-chlorophenyl)-1 H-pyrazol-5-amine as follows. To a solution of 2-(4-chlorophenyl)acetonitrile (15.0 g, 98.95 mmol) in THF was added NaH (60%) (4.73 g, 118.38 mmol) portionwise at room temperature. To the above mixture initially 2 mL of ethyl 2-phenylacetate was added and the mixture was warmed to 40°C for 10 min. It was cooled in an ice bath, and after the initiation of the reaction, the remaining ethyl 2-phenylacetate (15.35 mL), a total of 17.35 mL (108.84 mmol), was added dropwise. The ice bath was removed and stirring continued at room temperature for 3.5 h. At the end of this period the reaction mixture was quenched with aqueous NH<sub>4</sub>Cl solution (20 mL) and the pH was adjusted to 3 by adding 3N HCl. The mixture was partitioned with ethyl acetate (150 mL). The aqueous layer was extracted with ethyl acetate (50 mL). The combined ethyl acetate layer was washed with brine, dried (Na<sub>2</sub>SO<sub>4</sub>), filtered and solvent was evaporated to dryness under reduced pressure to afford 2-(4-chlorophenyl)-3-oxo-4-phenyl-butanenitrile in quantitative yield. This product was used for the next step without further purifications. The crude 2-(4-chlorophenyl)-3-oxo-4-phenyl-butanenitrile was dissolved in toluene (150 mL). To the above solution was added acetic acid (31.12 mL, 544.22

mmol) followed by hydrazine hydrate (14.40 mL, 296.85 mmol) dropwise. The reaction mixture was refluxed for 16 h. At the end of this period, it was cooled to room temperature and solvent and excess reagents were removed under reduced pressure. The residue was neutralized with saturated NaHCO<sub>3</sub> solution, and the separated solid was filtered and washed with water (3x50 mL) and dried under vacuum at 50°C for 10h to afford title product (22.0 g, 78%). <sup>1</sup>H-NMR (400 MHz, DMSO-*d*6) 7.36 (d, *J*= 8.4 Hz, 2H), 7.29-7.17 (m, 4H), 7.16-7.10 (m, 1H), 7.04 (d, *J*= 8.5, 2H), 4.57 (bs, 2H), 3.87 (s, 2H). 3-benzyl-4-(4-chlorophenyl)-1*H*-pyrazol-5-amine and ethyl 3-(4-nitrophenyl)-3-oxo-propanoate were then refluxed in acetic acid for 16 h.



**Scheme: Synthesis of 2-benzyl-3-(4-chlorophenyl)-5-(4-nitrophenyl)-4H-pyrazolo[1,5- a]pyrimidin-7-one (NAV-2729).** i = Ethyl 3-(4-nitrophenyl)-3-oxo-propanoate, acetic acid, 120 °C, 16 h.

To a suspension of 3-benzyl-4-(4-chlorophenyl)-1*H*-pyrazol-5-amine (3.0 g, 10.6 mmol) in acetic acid (50 mL) was added ethyl 3-(4-nitrophenyl)-3-oxo-propanoate (2.5 g, 10.6 mmol) at room temperature. The reaction mixture was heated at 120 °C, 16 h. At the end of this period the mixture was cooled to room temperature and the precipitate was collected, filtrated, and washed with acetic acid. The filter cake was triturated with 20% ethyl acetate in hexanes to provide NAV-2729 (3.40 g, 70%). TLC (CH<sub>2</sub>Cl<sub>2</sub>:MeOH, 95:5 v/v): RF = 0.46; <sup>1</sup>H-NMR (400 MHz, DMSO-*d*6) (Figure S6M) δ 12.32 (s, 1H), 8.35 (d, *J*=8.5 Hz, 2H), 8.00 (d, *J*= 7.8 Hz, 2H), 7.50-7.34 (m, 4H), 7.28-7.00 (m, 5H), 6.10 (s, 1H), 4.00 (s, 2H); <sup>13</sup>C- NMR (400 MHz, DMSO-*d*6) (Figure S6N) δ 32.5, 96.4, 123.4, 126.1, 128.2, 128.4, 129.3, 129.7, 131.7, 131.8, 138.5, 148.6, 155.6; HRMS (Figure S6O) (FT-ESI) (*m/z*): [M + H]<sup>+</sup> calculated for C<sub>25</sub>H<sub>18</sub>ClN<sub>4</sub>O<sub>3</sub> 457.1061, found 457.1078; HPLC (Figure S6P) purity, 96.9% (*t*R = 8.54 min).

### Molecular Modeling

Molecular modeling was performed using program package ICM-Pro (MolSoft, LLS, San Diego, CA) that includes modules for homology modeling, docking and virtual ligand screening. Homology model of N-terminally truncated ARF6 (Δ13) structure was built using ARF1 (Δ17) template extracted from a crystal structure of ternary ARF1 (Δ17)-GDP ARNO complex with inhibitor brefeldin A (Protein Data Bank ID 1S9D) (Renault et al., 2003). Then ARF1 structure in the ternary complex was replaced with the homology model of ARF6 and brefeldin A (BFA) was removed from the complex. Inhibitor NAV-2729 was docked into a binding site at the interface between ARF6 and ARNO. The preliminary model of ARF6-ARNO complex with NAV-2729 was refined using a binding site side chain optimization procedure available with ICM-Pro program.

### Statistical analyses

Statistical analyses were performed using GraphPad Prism 6.0f. When two groups were being compared and the data appeared to be normally distributed and the variances were approximately equal, the Student's t test was used. Welch's correction was applied when the variances were not equal or the number of data points was significantly different. When multiple t tests were performed on groups of similar data, a Holm-Sidak multiple t test analysis was used. When multiple treatment groups were being compared to a single control and the data were normally distributed, one-way ANOVA with Dunnett's multiple comparisons test was performed. When multiple groups were being compared and each group was compared to all other groups and the data were normally distributed, one-way ANOVA with Tukey's multiple comparisons test was performed. When the data did not appear to be normally distributed, the Mann-Whitney U test was used. For categorical data where two treatment groups are classified by two different outcomes, Fisher's exact test was used. For statistical analyses of immunoblots, the density of each band was normalized to an internal control protein and then the ratio of the normalized density of the band from the experimental treatment to the normalized density of the paired control treatment band was obtained. Because these values are ratios, geometric means and 95% confidence intervals were calculated and the ratios were plotted on a logarithmic scale to determine significance.

## **SUPPLEMENTAL REFERENCES**

McEwen, D. P., Gee, K. R., Kang, H. C., and Neubig, R. R. (2001). Fluorescent BODIPY-GTP analogs: real-time measurement of nucleotide binding to G proteins. *Anal Biochem* 291, 109-117.